Red Emitting Phenothiazine Dendrimers Encapsulated 2-{2-[2-(4-Dimethylaminophenyl)vinyl]-6-methylpyran-4-ylidene}malononitrile Derivatives

Go Woon Kim,† Min Ju Cho,† Young-Jun Yu,† Zee Hwan Kim,† Jung-Il Jin,† Dong Young Kim,‡ and Dong Hoon Choi*,†

Department of Chemistry, Center for Electro- & Photo-responsive Molecules, Korea University, Seoul 136-701 Korea, and Opto Electronic Materials Research Center, Korea Institute of Science and Technology, Seoul, 136-791 Korea

Received August 6, 2006. Revised Manuscript Received October 27, 2006

New red light emitting dendrimers were synthesized by reacting 2-[2-(2-{4-[bis(6-hydroxyhexyl)amino]-phenyl}vinyl)-6-methylpyran-4-ylidene]malononitrile (**15**) or 2-[2,6-bis(2-{4-[bis(6-hydroxyhexyl)amino]-phenyl}vinyl)pyran-4-ylidene]malononitrile (**16**) with 3,5-bis{3,5-bis[2-(10-hexyl-10*H*-phenothiazin-3-yl)vinyl]benzyloxy}benzoic acid (**9**) by DCC catalyzed esterification. Two kinds of red emitting core dyes capable of electronic excitation via Förster energy transfer were encapsulated by phenothiazine (PTZ) dendrons. Photoluminescence (PL) studies of the dendrimers demonstrated that, at the high density of a PTZ dendron, a significantly high-energy transfer to the core is achieved as a result of the large overlap between the absorption spectrum of a core emitting dye and the PL spectrum of the PTZ dendron. The electroluminescence (EL) spectra of multilayered devices showed red emissions, similar to those observed in the PL spectra of dendrimer thin films. The multilayered devices showed a luminance of 490 cd/m^2 at 254 mA/cm^2 (11.4 V) for **17** and 210 cd/m^2 at 321 mA/cm^2 (11.7 V) for **18**. The EL quantum efficiency of **18** ($\eta_{ext} = 0.56\%$) increased with an increase in the density of a light-harvesting PTZ dendron. The larger dendrimer, **18** bearing a more polar emitting core exhibited a considerably pure red emission with CIE 1931 (Commission International de L'Eclairage) chromaticity coordinates of $x = 0.64$, $y = 0.34$.

Introduction

Recently, semiconducting organic materials have attracted considerable interest as good candidate materials in electronics and optoelectronics.[1−5] Among their many application fields, electroluminescence (EL) devices using small molar mass organic materials have become the most popular technology that have already been employed in practical applications such as flat-panel or flexible display devices.[6−15]

Besides the utilization of fluorescent small molecules for organic light emitting diodes (OLEDs), polymer light emitting materials, which provide an overall device performance inferior to that provided by small molecules, can also be used to provide a fast response, high brightness, low driving voltage, ease of device fabrication, and good processability.[16−24]

Recently, functional dendrimers have been proposed to prepare multichromophoric material systems that possess

* Corresponding author. E-mail: dhchoi8803@korea.ac.kr.
† Korea University.
‡ Korea Institute of Science and Technology.

(1) Friend, R. H.; Gymer, R. W.; Holmes, A. B.; Burroughes, J. H.; Marks, R. N.; Taliani, C.; Bradley, D. D. C.; Dos, Santos, D. A.; Brédas, J. L.; Lögdlund, M.; Salaneck, W. R. *Nature* **1999**, *397*, 121−128.
(2) Dimitrakopoulos, C. D.; Malenfant, P. R. L. *Adv. Mater.* **2002**, *14*, 99−117.
(3) Crone, B.; Dodabalapur, A.; Ln, Y. Y.; Filas, R. W.; LaDuca, Z. Bzo, A.; Sarpeshkar, R.; Katz, H. E.; Li, W. *Nature* **2000**, *403*, 521−523.
(4) Sirringhaus, H.; Tessler, N.; Friend, R. H. *Science* **1998**, *280*, 1741−1744.
(5) Halls, J. J. M.; Arias, A. C.; MacKenzie, J. D.; Wu, W.; Inbasekaran, M.; Woo, E. P.; Friend, R. H. *Adv. Mater.* **2000**, *12*, 498−502.
(6) Adachi, C.; Baldo, M. A.; Forrest, S. R. *Appl. Phys. Lett.* **2000**, *87*, 8049−8055.
(7) Hong, Z.; Liang, C.; Li, R.; Li, W.; Zhao, D.; Fan, D.; Wang, D.; Chu, B.; Zang, F.; Hong, L.-S.; Lee, S.-T. *Adv. Mater.* **2001**, *13*, 1241−1245.
(8) Sun, P.-P.; Duan, J.-P.; Shih, H.-T.; Cheng, C.-H. *Appl. Phys. Lett.* **2002**, *81*, 792−794.
(9) Liang, F.; Zhou, Q.; Cheng, Y.; Wang, L.; Ma, D.; Jing, X.; Wang, F. *Chem. Mater.* **2003**, *15*, 1935−1937.
(10) Sun, M.; Xin, H.; Wang, K.-Z.; Zhang, Y.-A.; Jin, L.-P.; Huang, C.-H. *Chem. Commun.* **2003**, 702−703.
(11) Sun, P.-P.; Duan, J.-P.; Lih, J.-J.; Cheng, C.-H. *Adv. Funct. Mater.* **2003**, *13*, 683−691.
(12) Fang, J.; Ma, D. *Appl. Phys. Lett.* **2003**, *83*, 4041−4043.
(13) Tang, C. W.; VanSlyke, S. A. *Appl. Phys. Lett.* **1987**, *52*, 913−915.
(14) Tang, C. W.; VanSlyke, S. A.; Chen, C. H. *Appl. Phys. Lett.* **1989**, *65*, 3610−3616.
(15) Burroughes, J. H.; Bradley, D. D. C.; Brown, A. R.; Marks, R. N.; Mackay, K.; Friend, R. H.; Burn, P. L.; Holmes, A. B. *Nature* **1990**, *347*, 539−541.
(16) Kraft, A.; Grimsdale, A. C.; Holmes, A. B. *Angew. Chem. Int. Ed.* **1998**, *37*, 402−428.
(17) Yang, Y.; Heeger, A. J. *Nature* (*London*) **1994**, *372*, 344−346.
(18) Yang, Z.; Sokolik, I.; Karasz, F. E. *Macromolecules* **1993**, *26*, 1188−1190.
(19) Yoon, C. B.; Moon, K. J.; Shim, H. K. *Macromolecules* **1996**, *29*, 5754−5755.
(20) Hsieh, B. R.; Antoniadis, H.; Bland, D. C.; Feld, W. A. *Adv. Mater.* **1995**, *7*, 36−39.
(21) Jiang, X. Z.; Register, R. A.; Killeen, K. A.; Thompson, M. E.; Pschenitzka, F.; Sturm, J. C. *Chem. Mater.* **2000**, *12*, 2542−2549.
(22) Wang, Y. Z.; Sun, R. G.; Meghdadi, F.; Leising, G.; Epstein, A. *J. Appl. Phys. Lett.* **1999**, *74*, 3613−3615.
(23) Friend, R. H.; Gymer, R. W.; Holmes, A. B.; Burroughes, J. H.; Marks, R. N.; Taliani, C.; Bradley, D. D. C.; Dos Santos, D. A.; Brédas, J. L.; Lögdlund, M.; Salaneck, W. R. *Nature* (*London*) **1999**, *397*, 121−128.

10.1021/cm0618493 CCC: $37.00
Published on Web 12/10/2006

unique molecular architecture and characteristics. It has been found that the photophysical properties of the core such as the absorption and emission behaviors can be fine-tuned by modifying the environment around the core.[25,26] In order to improve the EL efficiency, periphery-to-core energy transfer systems based on light harvesting π-conjugated dendrimers have often been prepared.[27−30] EL dendrimers exhibit a unique feature that is attractive for use in EL devices. The peripheral groups assist in core isolation as well as optimal geometry formation for an improved light harvesting property.[31−37] The site-isolation effect provided by bulky dendrons minimizes the undesired core−core interaction. Moreover, by systematically modifying the structures of a peripheral dendron, the overall energy transfer efficiency of EL devices can be optimized.

In this work, we report the synthesis and photophysical properties of two dendrimers (see Scheme 3) consisting of phenothiazine (PTZ) peripheral moieties and red emitting cores. We found that the electron-rich phenothiazine ring is an excellent light harvesting molecular dendritic wedge whose PL emission is well-suited to excite the red emitting core. Moreover, the nonplanar phenothiazine ring structure of the dendrimer restricts π-stacking aggregation, which prevents the detrimental pure singlet exciton recombination process.[38] Furthermore, we investigated the density effects of the PTZ moiety at a periphery on the PL and EL characteristics, which are discussed with references to possible mechanisms.

Experimental Section

Synthesis. Detailed synthetic procedures for all compounds and characterization data can be found in the Supporting Information.

Instrumental Analysis. ^{1}H NMR spectra were recorded on a Varian Mercury NMR 300 Hz spectrometer using deuterated chloroform or DMSO purchased from Cambridge Isotope Laboratories, Inc. ^{13}C NMR spectra were recorded using a Varian Inova-500 spectrometer. Elemental analysis was performed by using an EA1112 (Thermo Electron Corp.) elemental analyzer. High-resolution mass analysis was performed on a JMS-700 MStation mass spectrometer (JEOL, resolution 60,000, *m*/*z* range at full sensitivity 2400). MALDI-TOF analysis was performed on a Voyager-DE STR MADI-TOF (matrix; DHB) mass spectrometer.

Thermal properties were studied under a nitrogen atmosphere on a Mettler DSC 821^e instrument. The redox properties of the synthesized compounds were examined by cyclic voltammetry (model: EA161 eDAQ). The dendrimer thin films were coated on a platinum plate using chloroform as a solvent. The electrolyte solution employed was 0.10 M tetrabutylammonium hexafluorophosphate (Bu_4NPF_6) in a freshly dried acetonitrile or MC. The Ag/AgCl and Pt wire (0.5 mm in diameter) electrodes were utilized as reference and counter electrodes, respectively. The scan rate was at 50 mV/s.

Absorption and Photoluminescence Spectroscopy. Studying absorption and PL behavior, dendrimer films were fabricated on quartz substrates as follows. The solution (3 wt %) of each dendrimer in chloroform was filtered through an acrodisc syringe filter (Millipore 0.2 μm) and subsequently spin-cast on the quartz glass. The films were dried overnight at 80 °C for 48 h under vacuum.

Absorption spectra of film samples and of chloroform solution (concentration 1×10^{-5} mol/L) were obtained using a UV−vis spectrometer (HP 8453, PDA type) in the wavelength range of 190−1100 nm. PL spectra were recorded with an AMINCO-Bowman series 2 luminescence spectrometer.

For time-resolved PL analysis, all samples were excited by 400 nm pulses generated by frequency-doubling of the 800 nm 100 fs pulse from a mode-locked Ti: sapphire laser oscillator (Coherent, Chameleon). The PL kinetic profiles were recorded using a time-correlated single photon counting (TCSPC, EG&G Ortec) setup equipped with a photon-counting MCP−PMT (Hamamatsu) detector.

Electroluminescence Measurement. The multilayer diode have a structure of ITO/PEDOT:PSS (40 nm)/dendrimer (50 nm)/BCP (10 nm)/Alq_3 (40 nm)/LiF (1 nm)/Al (100 nm), respectively. The conducting PEDOT layer was spin-coated onto the ITO-coated glasses in an argon atmosphere. The emitting dendrimer layer then was spin-coated onto the thoroughly dried PEDOT layer using the solution (concentration 5 wt %) in monochlorobenzene.

For multilayer devices, 2,9-dimethyl-4,7-diphenyl-1,10-phenanthroline (BCP) and tris(8-hydroxyquinoline)aluminum (Alq_3) layer were vacuum-deposited using a VPC-260 (ULVAC, Japan) vacuum coater and a CRTM-6000 thickness monitor (ULVAC, Japan) onto the emitting dendrimer layer. Finally, LiF (1 nm)/Al (100 nm) electrodes were deposited onto the Alq_3 layer under the same condition.

EL spectra of the synthesized compounds were also acquired on an AMINCO-Bowman series 2 luminescence spectrometer. I−V characteristics were measured using an assembly consisting of dc power supply (Hewlett-Packard 6633B) and a digital multimeter (Hewlett-Packard 34970A). Luminance was measured by using a Minolta LS-100 luminance meter. The thickness of the dendrimer was determined by a TENCOR P-10 surface profilometer.

When measuring the hole and electron mobilities of the two dendrimers, we fabricated thick sandwiched samples ($t = 3.2-4.3$ μm) using ITO and Al electrodes. Sandwich-type samples of ITO/dendrimer/Al (300 Å) were fabricated for TOF measurements. A

(24) (a) Chung, S.-J.; Kwon, K. Y.; Lee, S. W.; Jin, J.-I.; Lee, C. H.; Lee, C. E.; Park, Y. *Adv. Mater.* **1998**, *10*, 1112−1116. (b) Chung, S.-J.; Jin, J.-I.; Lee, C. H.; Lee, C. E. *Adv. Mater.* **1998**, *10*, 684−688. (c) Kim, K.; Hong, Y.-R.; Lee, S.-W.; Jin, J.-I.; Park, Y.; Sohn, B.-H.; Kim, W.-H.; Park, J.-K. *J. Mater. Chem.* **2001**, *11*, 3023−3030. (d) Lee, D. W.; Kwon, K. Y.; Jin, J.-I.; Park, Y.; Kim, Y. R.; Hwang, I. W. *Chem. Mater.* **2001**, *13*, 565−574. (e) Park, J. H.; Kim, K.; Hong, Y. R.; Jin, J.-I.; Sohn, B. H. *Macromol. Symp.* **2004**, *212*, 51−61. (g) Cha, S. W.; Jin, J.-I. *Synth. Met.* **2004**, *143*, 97−101.
(25) Kuwabara, Y.; Ogawa, H.; Inada, H.; Noma, N.; Shirota, Y. *Adv. Mater.* **1994**, *6*, 677−679.
(26) Wang, P. W.; Liu, Y. J.; Devadoss, C.; Bharathi, P.; Moore, J. S. *Adv. Mater.* **1996**, *8*, 237−241.
(27) Kwok, C. C.; Wong, M. S., *Chem. Mater.* **2002**, *14*, 3158−3166.
(28) Weil, T.; Reuther, E.; Müllen, K. *Angew. Chem., Int. Ed.* **2002**, *41* (11), 1900−1904.
(29) Adronov, A.; Malenfant, P. R. L.; Fréchet, J. M. J. *Chem. Mater.* **2000**, *12*, 1463−1472.
(30) (a) Furuta, P.; Brooks, J.; Thompson, M. E.; Fréchet, J. M. J. *J. Am. Chem. Soc.* **2003**, *125*, 13165−13172. (b) Furuta, P.; Fréchet, J. M. J., *J. Am. Chem. Soc.* **2003**, *125*, 13173−13181.
(31) Halim, M.; Pilow, J. N. G.; Samuel, I. D. W.; Burn, P. L. *Synth. Met.* **1999**, *102*, 922−923.
(32) Lo, S.-C.; Male, N. A. H.; Markham, J. P. J.; Magennis, S. W.; Burn, P. L.; Salata, O. V.; Samuel, D. W. *Adv. Mater.* **2002**, *14*, 975−979.
(33) Cornil J.; Beljonne, D.; Calbert, J-P.; Brédas, J.-L. *Adv. Mat*er. **2001**, *13*, 1053−1067.
(34) Satoh, N.; Cho, J.; Higuchi, M.; Yamamoto, K. *J. Am. Chem. Soc.* **2003**, *125*, 8104−8105.
(35) Cornil, J.; dos Santos, D. A.; Crispin, X.; Silbey, R.; Brédas, J.-L. *J. Am. Chem. Soc.* **1995**, *120*, 1289−1299.
(36) Deb, S. K.; Maddux, T. M.; Yu, L. *J. Am. Chem. Soc.* **1997**, *119*, 9079−9080.
(37) Pogantsch, A.; Wenzl, F. P.; List, E. J. W.; Leising, G.; Grimsdale, A. C.; Müllen, K. *Adv. Mater.* **2002**, *14*, 1061−1064.
(38) Krämer, C. S.; Zeitler, K.; Muller, T. J. J. *Org. Lett.* **2000**, *2*, 3723−3726.

Scheme 1. Synthesis of 9 (PTZ-Dendron)[a]

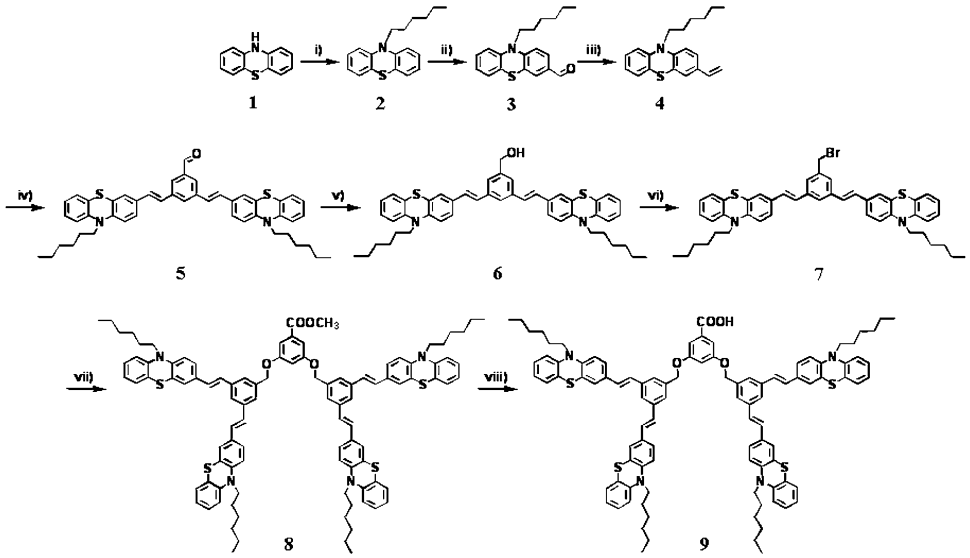

[a] Key: (i) phenothiazine, 1-bromohexane, NaH, DMF, rt; (ii) $POCl_3$, DMF, 1,2-dichloroethane, reflux; (iii) KO^{t}Bu, methyltriphenylphosphonium iodide, THF, rt; (iv) dibromobenzaldehyde, K_2CO_3, TBAB, $Pd(OAc)_2$, DMF, 100 °C; (v) $NaBH_4$, MeOH, THF, 60 °C; (vi) PBr_3, THF, 0 °C, rt. (vii) 3,5-dihydroxybenzoic acid methyl ester, K_2CO_3, 18-*crown*-6, acetone, reflux; (viii) KO^{t}Bu, THF, rt.

Scheme 2. Synthetic Procedure of 15 and 16[a]

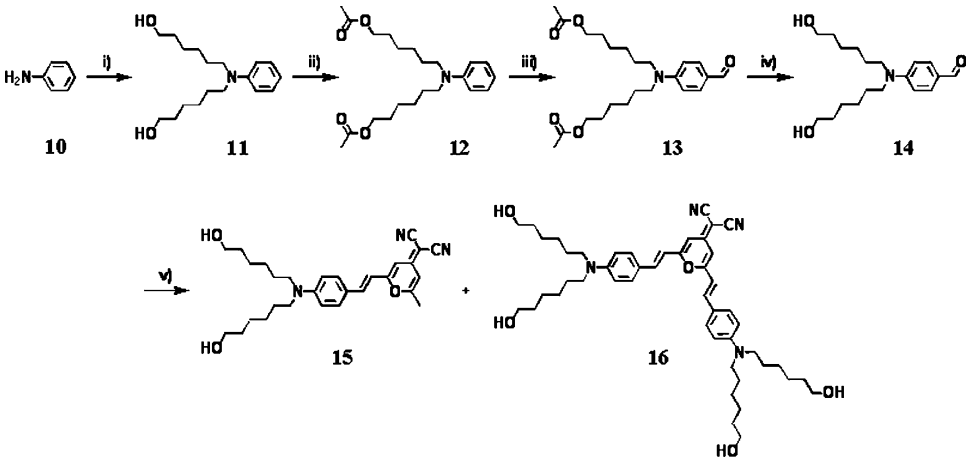

[a] Key:(i) 6-chlorohexan-1-ol, K_2CO_3, KI, DMF, 140 °C; (ii) Py, Ac_2O, MC, reflux; (iii) $POCl_3$, DMF, 1,2-dichloroethane, reflux; (iv) KOH, THF, reflux; (v) 2-(2,6-dimethylpyran-4-ylidene)malononitrile, piperidine, 1-propanol, reflux.

transient photocurrent was measured using a commercial TOF setup (OPTEL TOF-401), equipped with a nitrogen laser (λ = 337 nm, pulse duration = 600 ps) and recorded by a digital oscilloscope (Tektronix TDS3054B). The induced photocarriers were moved by the applied voltage between two electrodes, and the decay time of the electric current due to the photocarriers drifting through a dendrimer film was determined after light illumination was switched off. In this experiment, by changing the polarity of the applied voltage, the hole and electron mobilities can be measured individually. Measurement of EL device performance and TOF were performed in Center for Organic Light Emitting Diode located in Seoul National University, Korea.

Results and Discussion

General Properties of Dendrimers. The synthetic routes to prepare **9**, **15**, and **16** and two dendrimers (**17** and **18**) can be found in Schemes 1−3. The syntheses of the PTZ precursor compounds and **5** were reported in our previous work.[39,40] The synthesis of **5** was carried out by the Heck coupling reaction of **4** with dibromobenzaldehyde to produce a light harvesting peripheral dendron. The base-catalyzed hydrolysis produced 1-carboxylic acid substituted PTZ branched dendron (**9**) quantitatively. We synthesized two red emitting core dyes that contained either one dihexylaminophenyl donor or two donors (see Scheme 2). **15** and **16** were encapsulated with the PTZ dendrons. Eight PTZ groups were attached to two hydroxyl groups in the core **15** to yield a second generation dendrimer, **17**. Sixteen PTZ moieties were attached to four hydroxyl groups in **16** to yield **18**. Two reactions were conducted by DCC catalyzed esterification. The PTZ dendron and red emitting core were connected through a nonconjugated alkylene spacer in order to isolate the photophysical properties of the two moieties. The newly synthesized dendrimers are well soluble at room

(39) Cho, M. J.; Kim, J. Y.; Kim, J. H.; Lee, S. H.; Dalton, L. R.; Choi, D. H. *Bull. of the Kor. Chem. Soc.* **2005**, *26*, 77−84.
(40) Zhang, X. H.; Choi, D. H.; Choi, S.-H.; Ahn, K.-H. *Tetrahedron Lett.* **2005**, *46*, 5273−5276.

Scheme 3. Synthesis of 17 and 18[a]

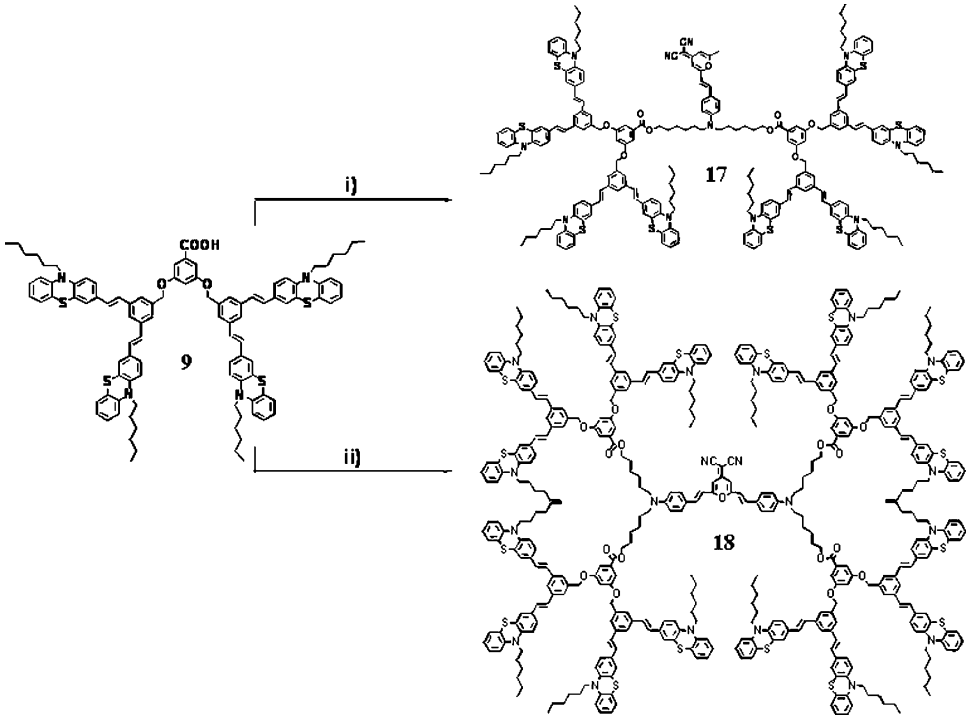

[a] Key: (i) **15**, DPTS, DCC, MC, rt; (ii) **16**, DPTS, DCC, MC, rt.

temperature in common organic solvents such as chloroform, THF, and chlorobenzene; they display good self-film forming properties.

The glass transition temperatures (T_g values) of the two dendrimers obtained by DSC are 78.5 °C for **17** and 83.5 °C for **18**. No discernible melting behavior up to 290 °C was observed in the DSC thermograms of these dendrimers.

Electrochemical Analysis and Absorption Spectroscopy: Molecular Energy Levels of the Compounds. Electrochemical analysis was performed to determine the redox ionization potentials of the synthesized compounds. The oxidation and reduction potentials are closely related to the HOMO and LUMO levels of the analyzed compounds. They can thus provide important information on the energy transfer process. Cyclic voltammograms were recorded on a film sample, and the potentials were obtained relative to an internal ferrocene reference (Fc/Fc^+). These CV scans in the range of −2.0 V to +2.0 V (vs Ag/AgCl) range show quasi-reversible oxidation peaks and irreversible reduction peaks. The dendrons **8**, **15**, and **16** in acetonitrile have one quasi-reversible oxidation (E_{ox}^{onset}) at 0.53, 0.74, and 0.72 V, respectively. Unfortunately, the reduction potentials were irreversible; therefore, we were unable to estimate their HOMO and LUMO energies accurately. In order to determine the LUMO levels, we combined the oxidation potential in CV with the optical energy band gap (E_g^{opt}) resulting from the absorption edge in an absorption spectrum. The HOMO levels of **8**, **15**, and **16** were determined to be −4.93, −5.32, and −5.12 eV, respectively (see Table 1) Since two dihexylaminophenyl donor groups are present in **16**, the HOMO level decreases, which is also observed in the HOMO levels of the other two dendrimers. Accordingly, the optical band gaps (E_g values) of the two dendrimers estimated from the UV−vis absorption edges are 2.24 eV for **17** and 2.07 eV for **18** (see Table 1). The optical band gap of **16** is slightly smaller than that of **15**. Because the core moiety is incorporated into the PTZ dendron via an alkylene unit, the overall band gap energy of each dendrimer was not affected significantly. Based on the measured energy levels of the compounds, we also confirmed the energy transfer facilitated from the PTZ dendron to the emitting core via the near-resonance of the energy levels of the energy donors and acceptors.

Table 1. Electrochemical and Absorption Properties of the Synthesized Compounds

sample	E_{ox}^{peak} (v)	E_{ox}^{onset} (v)	λ_{cutoff} (nm)	E_g^{opt} (eV)	HOMO (eV)	LUMO (eV)
8[a]	0.61	0.53	435	2.85	−4.93	−2.07
15[a]	0.84	0.74	546	2.27	−5.32	−2.87
16[a]	0.79	0.72	588	2.11	−5.12	−3.02
17[b]	1.37	0.87	554	2.24	−5.27	−3.08
18[b]	1.18	0.85	600	2.07	−5.25	−3.20

[a] Solution state. [b] Film state.

In order to deconvolute the absorption spectral properties of the two dendrimers, it is necessary to study the absorption property of the individual compounds (i.e., **8**, **15**, and **16**) separately. Figure 1 illustrates the absorption spectra of **8**, **15**, **16**, **17**, and **18** both in chloroform solutions (A) and in thin films (B) on fused silica glass. In the solution state, the PTZ dendron, **8**, has a maximum absorbance (λ_{max}^{abs}) at 376 nm with an extinction coefficient of 70 000 M^{-1} cm^{-1}. **15** and **16** exhibit a maximum absorbance at 482 and 497 nm with the extinction coefficients of 40 000 and 50 000 M^{-1} cm^{-1}, respectively. Each dendrimer exhibits distinct dual absorption maximas in the film state: one at around 386 nm and the other over a longer wavelength region (488 nm for **17**; 506 nm for **18**), which are attributed to the $\pi-\pi^*$

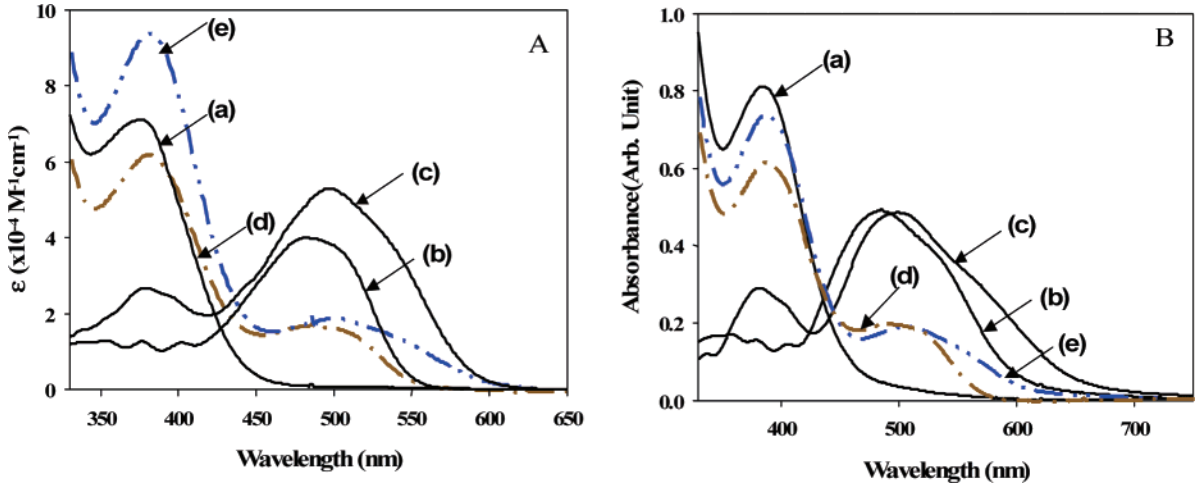

Figure 1. UV−vis absorption spectra of the PTZ dendron, core dyes, and the dendrimers. (A) Solution (concentration 1.0×10^{-5} M). The absorption coefficients of the two dendrimers were multiplied by 0.4 for a good comparison. (B) Film. Sample: (a) **8**, (b) **15**, (c) **16**, (d) **17**, (e) **18**.

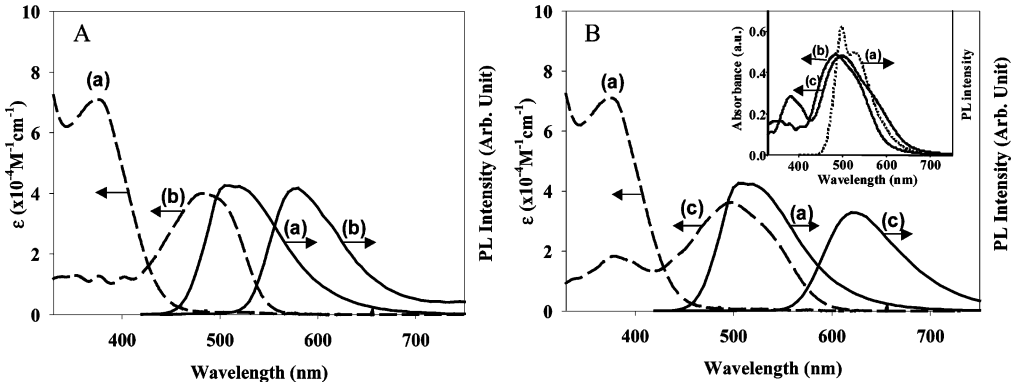

Figure 2. UV−vis absorption and PL spectra of **8** and the core dyes in a solution state. (A) (a) **8**, (b) **15**. (B) (a) **8**, (c) **16**. Inset: PL spectrum of **8** and absorption spectra of **15** and **16** in a film state. Sample: (a) **8**, (b) **15**, (c) **16**.

transitions of **8** and the transition from the core dye.[41,42]

Absorption and Photoluminescence Spectroscopy of the Two Dendrimers. The solution PL spectrum of **8** and the absorption spectrum of a core dye were superimposed and are represented in Figure 2 (A: **15**, B: **16**). From this figure, it is clearly evident that the emission spectrum of **8** and absorption spectrum of a core dye overlap favorably, which enables an efficient Förster energy transfer. Furthermore, a large energy difference between the absorption and PL maximum wavelength of the PTZ dendron over 100 nm assists in the minimization of the simultaneous excitation of the donor and acceptor moieties. This large energy difference is believed to originate from the large conformational change between the ground and excited states.

For a clear comparison, we have introduced the inset figure for the absorption spectra of **15** and **16** and emission spectrum of **8** using spin-cast films in Figure 2B. A larger overlap in **16** was observed, which implied a higher efficiency of energy transfer in **18**.

As shown in Figure 3A, the PL spectra of the dendrimers obtained in chloroform solutions at the excitation wavelength of 400 nm display two characteristic emission bands at about 500 and 580 nm for **17** and 620 nm for **18**. The weak emission at 500 nm is considered to originate from the PTZ dendron, and the strong emission at 580 nm is the result of the energy transfer from the PTZ dendron to the core dye, **15**. It is noted that the coupling of the PTZ moiety and the core dye to form an energy donor−acceptor complex nearly quenches the emission of the PTZ moiety. Furthermore, a more drastic PTZ emssion quenching and consequently an increased transfer efficiency are observed in the film sample.

As shown in Figure 3B, in the two dendrimer films, no emission from the PTZ dendron appears at 500 nm: however, only a red emission from the core units is observed ($\lambda_{em.}$ is 598 nm for **17** and 630 nm for **18**). These results can be explained by easier exciton migration or effective energy transfer from the PTZ dendron to the lower energy sites containing the core dye.[28,43,44] This implies that the energy transfer is much faster than the radiative decaying process

(41) (a) Chen, C. H.; Shi, J.; Tang, C. W. *Macromol. Symp.* **1997**, *125*, 1−48. (b) Jung, B.-J.; Yoon, C.-B.; Shim, H.-K.; Do, L.-M.; Zyung, T. *Adv. Funct. Mater.* **2001**, *11*, 430−434. (c) Kim, J. H.; Lee, H. *Chem. Mater.* **2002**, *14*, 2270−2275.

(42) Peng, Q.; Lu, Z.-Y.; Huang, Y.; Xie, M.-G.; Han, S.-H.; Peng, J.-B.; Cao, Y. *Macromolecules* **2004**, *37*, 260−266.

(43) Klärner, G.; Lee, J.-I.; Davey, M. H.; Miller, R. D. *Adv. Mater.* **1999**, *11*, 115−119.

(44) (a) Lee, J.-I.; Klaerner, G.; Davey, M. H.; Miller, R. D. *Synth. Met.* **1999**, *102*, 1087−1088. (b) Cho, N. S.; Hwang, D.-H.; Lee, J.-I.; Jung, B.-J.; Shim, H.-K. *Macromolecules* **2002**, *35*, 1224−1228. (c) Huang, J.; Niu, Y.; Yang, W.; Mo, Y.; Yuan, M.; Cao, Y. *Macromolecules* **2002**, *35*, 6080−6082. (d) Lee, J.-I.; Zyung, Y.; Miller, R. D.; Kim, Y. H.; Jeoung, S. C.; Kim, D. J. *J. Mater. Chem.* **2000**, *10*, 1547−1550.

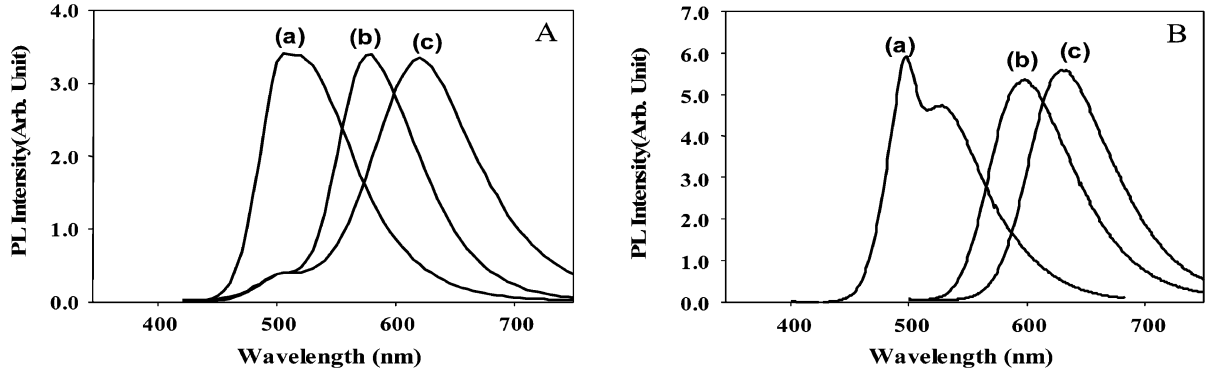

Figure 3. Photoluminescence (PL) spectra of the PTZ dendron and two dendrimers in a solution (A) and a film state (B). Sample: (a) **8**, (b) **17**, (c) **18**.

Table 2. Measured and Calculated Parameters for the Synthesized Compounds

				absorption			photoluminescence	
sample	dipole moment[a] (D)	T_m (°C)	T_g (°C)	solution (λ_{max}^{abs}, nm)	ϵ ($\times 10^{-4}$ $M^{-1}\,cm^{-1}$)	film (λ_{max}^{abs}, nm)	solution (λ_{max}^{PL}, nm)	film (λ^{PL}, nm)
8	2.7		71.0	376	7.0	385	505	498, 528
15	8.9	62.0		482	4.0	485	580	650
16	9.7	175.0		497	5.0	500	620	650
17			78.5	382, 485	15, 4.0	386, 488	500, 580	598
18			83.5	382, 498	24, 5.0	386, 506	500, 620	630

[a] Calculated values.

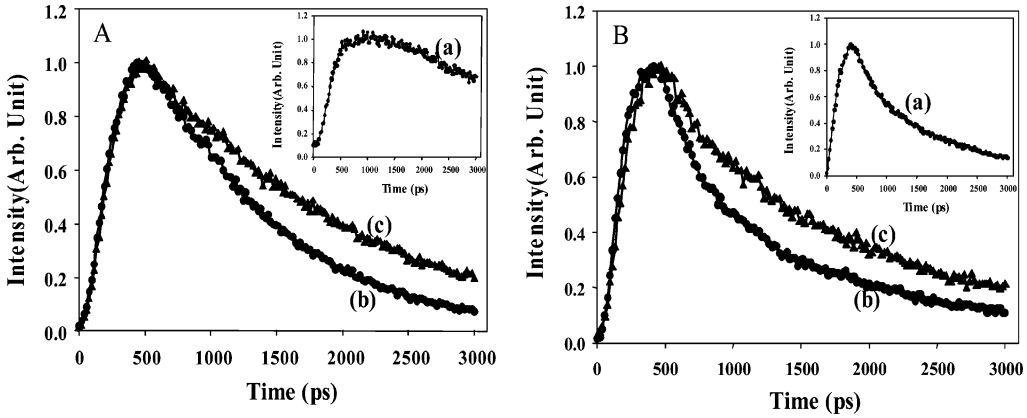

Figure 4. Time-resolved PL signal profiles of two dendrimers: (A) in a chloroform solution and (B) in a film state. Excitation at 400 nm and PL decay monitored at the corresponding PL maximum wavelength. Sample: (a) **8**, (b) **17**, and (c) **18**.

of the PTZ dendron. The parameters obtained from the absorption and PL studies are summarized in Table 2.

PL Kinetics for the Two Dendrimers. Time-resolved PL spectroscopy was employed to obtain additional information on the energy transfer dynamics of the two dendrimers. Figure 4A presents the PL decay profiles of **17** and **18** in chloroform solution at the detection wavelengths of 580 and 620 nm under an excitation at 400 nm. We also attempted to measure the PL emission at 500 nm originating from the PTZ dendron as well. However, the PL intensity at 500 nm was quenched substantially. Figure 4B displays the PL decay profiles of the dendrimer films monitored at 598 and 630 nm where the fluorescence is originated from the core moiety. The observed decay profiles fitted well with the single- or double-exponential decay functions for calculating the life time.

In Table 3, the fitted results of the analyses are summarized for the PTZ dendron and the dendrimer samples either in a solution or in a solid film. Figure 4A,B and Table 3 clearly demonstrate that the PL decaying rate of the PTZ dendron (**8**) is smaller than or comparable to those of the core dyes both in solution and the film state.

Table 3. PL Decay Lifetime of 8, 17, and 18 in a Solution and in a Film State

	λ_{det} (nm)		lifetime, τ (ps)	
sample	solution	film	solution[a,b]	film[a]
8	528	505	4146	1047
17	580	598	1038	655
18	620	630	1661	1013

[a] Uncertainty is ± 5% of the measured value. [b] Average lifetime of the two-exponential decay. λ_{det} (nm) = detecting wavelength.

On close examination, it is observed that the PL decay in a solution state shows two decay components. This is likely to occur due to the minor simultaneous excitation and the decay channel of the PTZ dendrons under an excitation at 400 nm, in addition to the major emission channel from the core dye *via* energy transfer from the PTZ dendron.

Figure 4B displays the PL decay profiles of **17** and **18** in thin films. In contrast to the solution sample, the PL decay for a thin film exhibits a monoexponential behavior. This is

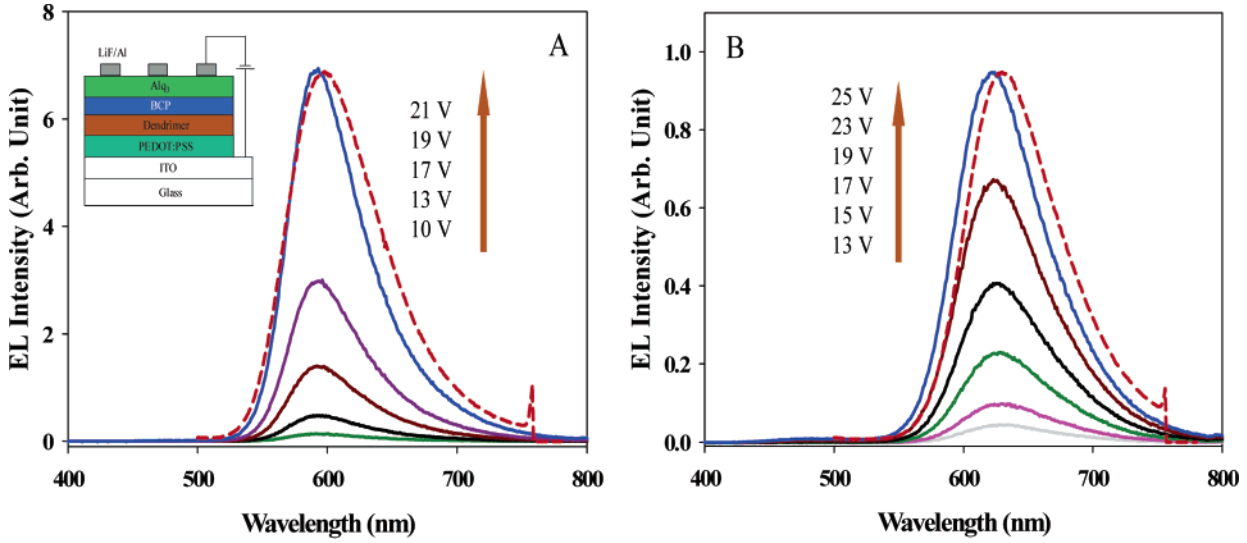

Figure 5. EL spectra of multilayered devices. (A) **17**. (B) **18**. Dotted line: corresponding PL spectrum in a film state.

due to the negligible PTZ donor emission and also due to the increased efficiency of energy transfer on solid formation. It is considered that the enhanced energy transfer originates from the high density and restricted conformation of the molecules in a solid, which tends to fix the spatial locations of the PTZ and core dyes at a more favorable geometry for energy transfer. The longer lifetime (1013 ps) of the larger dendrimer at 630 nm is mainly because of a higher shielding effect provided by a larger number of PTZ dendrons than those in **17**.

The dendrimer film samples exhibit much smaller PL lifetimes when compared with those of the chloroform solutions. The reduction in the excited-state lifetime of the films is due to the various fast radiative and nonradiative decay channels available for the solid-state samples in solid states, such as exciton trapping by defect sites via enhanced interchain interactions.[33,35,45]

Electrical and Electroluminescence Properties. We used two dendrimers for light emitting diodes (LEDs) as the emissive materials in multilayered devices. Poly(ethylene dioxythiophene):poly(styrene sulfonic acid) (PEDOT:PSS) thin film was deposited on indium tin oxide (ITO) as the anode for facilitating hole injection and the dendrimer was coated on it as an emissive layer. A thin film of 2,9-dimethyl-4,7-diphenyl-1,10-phenanthroline (BCP) with a thickness of 10 nm was subsequently vapor deposited on the dendrimer as a hole blocking material to confine exciton recombination and limit the loss of the faster moving holes to the cathode.[46,47] This was followed by the sequential deposition of a 40 nm electron injection layer of tris(8-hydroxyquinoline) aluminum (Alq_3)[48] and a LiF(1 nm)/Al electrode sequentially. We found that the EL device with BCP/Alq_3 layers were much more efficient than those without these layers.

Figure 5 shows the EL emission spectra of devices with **17** (A) and **18** (B) at varying forward bias voltages. The PL spectrum of each dendrimer is also indicated by a dotted line in the figures. No trace of emission from the Alq_3 layer was observed in the two spectra. The EL spectra are quite similar to the PL spectra, suggesting that the same excited-state species is responsible for both the PL and EL emissions.

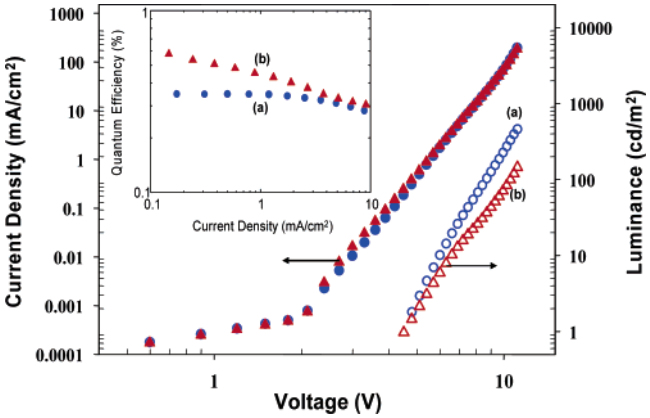

Figure 6. Dependence of current density and luminance on the electric field, Inset: external quantum efficiency of a multilayered EL device with the current density. Sample: (a) **17** (circle), (b) **18** (triangle).

At all forward bias voltages, only the characteristic orange-red or red emissions of **17** and **18** with a maximum EL emission at 590 and 622 nm are observed. As the voltage increases, the emission mainly originates from the core emitting dyes. By comparing the variation of the λ_{max}^{EL} precisely, we were able to observe that the smaller dendrimer **17** shows a slight blue-shift by 10 nm ($\Delta\lambda_{max}^{EL}$ from 10 V to 21 V). On the other hand, the stability of the λ_{max}^{EL} for **18** is much better, exhibiting a variation of only 5 nm variation in the voltage range of 13−25 V. This could be attributed to the higher shielding effect with the higher density of the PTZ dendron in **18** and reduction in the intermolecular interaction between the core dyes.

Another characteristic feature of these EL spectra is that no leakage of holes into the BCP and Alq_3 layers diminishes the blue/green emission. This indicates that the exciton

(45) Samuel, I. D. W.; Crystall, B.; Rumbles, G.; Burn, P. L.; Holmes, A. B.; Friend. R. H. *Chem. Phys. Lett.* **1993**, *213*, 472−478.
(46) Halim, M.; Samuel, I. D. W.; Pillow, J. N. G.; Monkam, A. P.; Burn, P. L. *Synth. Met.* **1999**, *102*, 1571−1574.
(47) (a) Baldo, M. A.; Lamansky, S.; Burrows, P. E.; Forrest, S. R.; Thompson, M. E. *Appl. Phys. Lett.* **1999**, *75*, 4. (b) Tsutsui, T.; Yang, M. J.; Masayuki, M.; Nakamura, Y.; Wanabe, T.; Tsuji, T.; Fukuda, Y.; Wakimoto, T.; Miyaguchi, S. *Jpn. J. Appl. Phys.* **1999**, *38*, L1502.

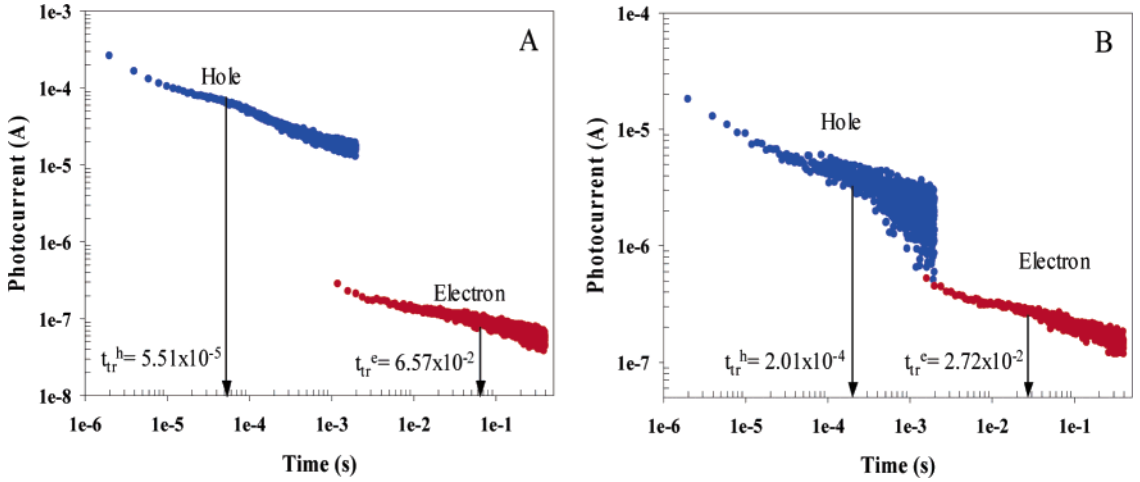

Figure 7. Double logarithmic plots of transient photocurrent at 25 °C. Arrows indicate the transit time for each carrier drifting. ITO/dendrimer (3.2−4.3 μm)/Al (∼100 nm). (A) **17**. (B) **18**.

recombination zone is located in the emitting dendrimer layer. BCP is crucial for confining the charge recombination in the emissive layer of the dendrimer and preventing from undesired emissions from Alq_3. When the EL spectrum was converted into chromaticity coordinates on the CIE 1931 diagram, a highly saturated red emission from **18** was obtained ($x = 0.64$, $y = 0.34$), which is almost consistent with the National Television System Committee (NTSC) standard for red color ($x = 0.67$, $y = 0.33$). The coordinates of the smaller dendrimer **17**, which displays orange-red emissions, are $x = 0.58$ and $y = 0.41$.

The current−voltage and luminance−voltage curves of the two dendrimers are shown in Figure 6. The turn-on voltages (electric fields) of the two LEDs were in the range of 4.7−4.8 V. The voltages were almost identical due to the close proximity of the HOMO energy levels of the two dendrimers. The maximum brightness of the LEDs was in the range of 490 cd/m^2 (at 254 mA/cm^2) for **17** to 201 cd/m^2 (at 321 mA/cm^2) for **18**. The larger dendrimer had a lower luminance value as an effect of the longer emission wavelength of the core.[49] The inset figure displays the dependence of the external quantum efficiency on the current density for two dendrimer EL devices. The maximum external quantum efficiencies of **17** and **18** EL devices were determined to be 0.35% (at 0.31 mA/cm^2, 0.58 cd/A, 0.38 lm/W and 436 cd/m^2) and 0.58% (at 0.24 mA/cm^2, 0.40 cd/A, 0.29 lm/W and 175 cd/m^2). It should be noted that the smaller dendrimer, **17** device clearly showed a lower efficiency than the larger dendrimer **18** device unequivocally at a relatively lower current density. In a higher electric field, a quenching effect was induced that was observed to reduce the efficiency.

It is also well-known[50] that a balance in the mobility of the opposite carriers is important for achieving improved efficiencies of EL devices. Although the difference between the external quantum efficiencies is not so significant, it is worth proving this by a precise hole and electron mobility measurement. This could be confirmed by the direct measurements of the electron/hole mobilties using the TOF technique.

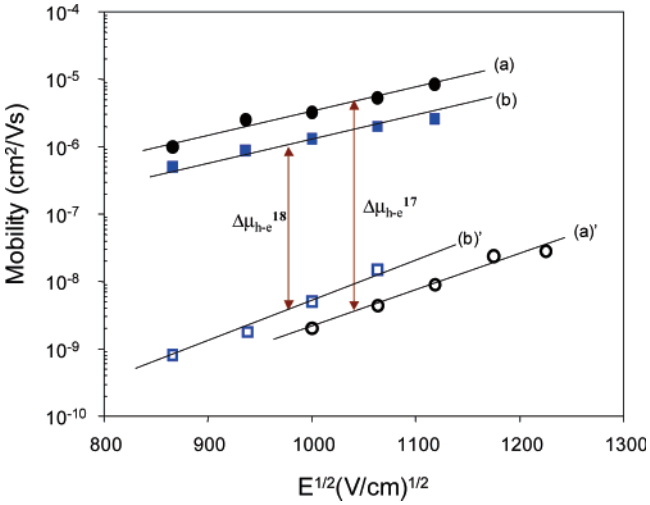

Figure 8. Electric field dependence of carrier mobilities for two dendrimers. Hole mobility: (a) **17**, (b) **18**. Electron mobility; (a)′ **17**, (b)′ **18**.

We investigated the transient photocurrent of the dendrimer sample with a 3.2−4.3 μm electrode distance by measurement in the electric field. The optical densities of **17** and **18** films were 41 100 and 43 300 cm^{-1} at a wavelength of 337 nm from the N_2 laser. This result shows that the carrier transport of **17** is slightly more dispersive than that of **18**. The double logarithmic plots to determine the transit time (t_τ) are illustrated in Figure 7. The transit time was determined by using the software loaded in the instrument.

In Figure 7, the representative transient photocurrents from the drift of the hole and electron at 113 MV/m are shown. A larger difference between the hole and electron transit time in **17** is noticed in comparison to that in **18**. Such a difference between the transit times implies the presence of unbalanced

(48) (a) Kelper, R. G.; Beeson, P. M.; Jacobs, S. J.; Anderson, R. A.; Sinclair, M. B.; Valencia, V. S.; Cahill, P. A. *Appl. Phys. Lett.* **1995**, *66*, 3618−3620. (b) Wu, C. C.; Chun, J. K. M.; Burrows, P. E.; Sturm, J. C.; Thompson, M. E.; Forrest, S. R.; Register, R. A. *Appl. Phys. Lett.* **1995**, *66*, 653−655. (c) Hosokawa, C.; Tokailin, H.; Higashi, H.; Kusumoto, T. *Appl. Phys. Lett.* **1992**, *60*, 1220−1222.

(49) Chen, C-T. *Chem. Mater.* **2004**, *16*, 4389−4400.

(50) (a) Heeger, A. J.; Parker, I. D.; Yang, Y. *Synth. Met.* **1994**, *67*, 23−29. (b) Baigent, D. R.; Greenham, N. C.; Grüner, J.; Marks, R. N.; Friend, R. H.; Moratti, S. C.; Holmes, A. B. *Synth. Met.* **1994**, *67*, 3−10. (c) Jang, J. W.; Lee, C. E.; Lee, D. W.; Jin, J.-I. *Solid State Commun.* **2004**, *130*, 265−268.

carrier flows, rendering the recombination region close to the cathode, where a high density of quenching centers or carrier traps is located. For instance, we determined the transit times and drifting hole mobilities of **17** and **18** at 113 MV/m as 5.51×10^{-2} ms (5.32×10^{-6} cm^2/Vs) and 2.01×10^{-1} ms (2.42×10^{-6} cm^2/Vs), respectively. Using the same method, we also measured the hole/electron mobilities of the two dendrimers with the applied electric field.

In Figure 8, the hole and electron drifting mobilities are plotted as a function of the applied voltages. While the hole mobility in **18** is much lesser than that in **17** and the electron mobility is more than two times than that in **17**. Thus, **18** exhibits a considerably improved balancing of the charge carrier transport than **17**, which functions to move the radiative region away from the interface where the quenching centers are abundant. This explains the enhanced external quantum efficiencies in **18**.

Conclusion

We have described the synthesis and characterization of noble PTZ branched dendrimers bearing red emitting moieties as a core. Although the dendrimers displayed simultaneous PL emissions at 500 and 580 nm for **17** from both structural components in a chloroform solution, they exhibited quite a significant suppression of the PL intensity from the PTZ dendron in the solid state.

We also observed that the light emission of the LED devices fabricated with the dendrimers was solely from the components containing the low-band gap structural material (i.e., the red emitting core). This is attributed to the efficient energy transfer or exciton migration from the PTZ dendron to the acceptor moieties. The molecular architecture of the dendrimer with a PTZ dendron and a core unit suppresses an undesired short wavelength emission and leads to a stabilized emission from these dendrimers due to rapid energy transfer from the light harvesting dendron to the core unit.

When we fabricate multilayered devices by inserting a thin layer of electron injecting Alq_3 layer and hole blocking BCP layer between the emitting dendrimer layer and the cathode, we observe a significant improvement in the EL efficiencies. The EL quantum efficiency of dendrimer devices largely increases with increasing the concentration of the light harvesting PTZ moiety. This was clearly demonstrated by the TOF experiment. Our work unambiguously demonstrates the complete utilization of the dendrimers that take advantage of the excited energy transfer fully utilized for fabricating better EL devices.

Acknowledgment. This work was supported by the Korea Science and Engineering Foundation through CRM of Korea University and the Seoul R&BD Program (2005-2006). Particularly, D.H.C. thanks LG-Philips LCD for financial support (Grant M1-0302-00-0027, 2005).

Supporting Information Available: Detailed procedures for the synthesis, spectrometric characterization of the compounds reported, and double logarithmic plots of transient photocurrent. This material is available free of charge via the Internet at http://pubs.acs.org.

CM0618493